Energy Conversion and Management 123 (2016) 56–70

Contents lists available at ScienceDirect

Energy Conversion and Management

journal homepage: www.elsevier.com/locate/enconman

Multidisciplinary design optimization of large wind turbines—Technical, economic, and design challenges

Turaj Ashuri [a,*,1], Michiel B. Zaaijer [b,2], Joaquim R.R.A. Martins [c,3], Jie Zhang [a,2]

[a] Department of Mechanical Engineering, University of Texas at Dallas, Richardson, TX, USA
[b] Department of Aerodynamics and Wind Energy, Delft University of Technology, Delft, ZH, The Netherlands
[c] Department of Aerospace Engineering, University of Michigan, Ann Arbor, MI, USA

ARTICLE INFO

Article history:
Received 6 May 2016
Received in revised form 31 May 2016
Accepted 1 June 2016

Keywords:
Upscaling
Levelized cost of energy
Wind turbine design
Annual energy production
Design optimization

ABSTRACT

Wind energy has experienced a continuous cost reduction in the last decades. A popular cost reduction technique is to increase the rated power of the wind turbine by making it larger. However, it is not clear whether further upscaling of the existing wind turbines beyond the 5–7 MW range is technically feasible and economically attractive. To address this question, this study uses 5, 10, and 20 MW wind turbines that are developed using multidisciplinary design optimization as upscaling data points. These wind turbines are upwind, 3-bladed, pitch-regulated, variable-speed machines with a tubular tower. Based on the design data and properties of these wind turbines, scaling trends such as loading, mass, and cost are developed. These trends are used to study the technical and economical aspects of upscaling and its impact on the design and cost. The results of this research show the technical feasibility of the existing wind turbines up to 20 MW, but the design of such an upscaled machine is cost prohibitive. Mass increase of the rotor is identified as a main design challenge to overcome. The results of this research support the development of alternative lightweight materials and design concepts such as a two-bladed downwind design for upscaling to remain a cost effective solution for future wind turbines.

1. Introduction

Over the last decades, the cost of wind generated electricity has experienced a continuous reduction thanks to research and development [1–3]. This cost reduction has enabled wind energy to become more viable, and today wind energy is one of the most affordable forms of renewable energy [4–7]. Upscaling has been performed as the basis to enable this cost reduction [8,9]. The development of larger wind turbines is supported by several factors, such as higher energy capture per area land use, and cost reduction per rated mega Watt (MW) capacity with fewer larger machines for the same installed capacity. Therefore, turbine size is often considered as a merit index for technology progress and development [10–13].

Despite significant technological improvements, the average cost of wind generated electricity is higher than that from traditional energy resources such as coal and natural gas [14,15], and it is subject to a larger variability [16–18]. It is not clear whether further upscaling beyond the existing 5–7 MW range is both technically feasible and economically attractive. Typically, analytic scaling laws, and extrapolation of existing wind turbine data are used to develop different scaling trends. These scaling trends are needed to investigate the impact of size on the technical design and the associated cost [19–21].

However, analytic scaling laws are not capable of providing accurate realizations of large scale wind turbines. This is related to the simple formulation of analytic scalings, which makes them suitable for the conceptual design phase. As the size increases beyond the few MW range, the pronounced interaction between disciplines such as aerodynamics, structures, and controls, as well as the complex system dynamics of more flexible components, presents design challenges [22–25]. Therefore, it is questionable whether analytic scaling can model the complex scaling behavior of large wind turbines to accurately quantify the impact of size.

Extrapolation of the existing wind turbine data also introduces large uncertainties in the design, and it is of limited use for this research. Additionally, distributed model properties can not be extracted from existing data trends to take into account the wide range of design solutions from every different manufacturer present in the trends.

* Corresponding author.
E-mail address: turaj.ashuri@utdallas.edu (T. Ashuri).
[1] Visiting assistant professor.
[2] Assistant professor.
[3] Professor.

http://dx.doi.org/10.1016/j.enconman.2016.06.004
0196-8904/

To address these problems, this research uses 5, 10, and 20 MW wind turbines that are developed using multidisciplinary design optimization (MDO) [26] with a similar design concept and design assumptions for all sizes. This enables the incorporation of all important disciplines and components for making reliable scaling trends that are needed to accurately quantify the technical and economical aspects of upscaling.

Compared to classical upscaling methods, the same design assumptions reduce the scattering of the data points used for scaling trends. It may also help to identify which aspects of the chosen concept have strong or weak scaling behavior. Therefore, using the design data of the developed 5, 10, and 20 MW turbines, loading, mass, and cost trends are constructed and used to predict what exactly happens to the design and its associated costs as the size increases. This enables a more accurate prediction of the economic viability of upscaling, and the identification of the design challenges that need to be overcome to achieve that viability.

The remainder of this paper is organized as follows. First, a brief overview of the two classical upscaling methods is presented. Then, the development of the 5, 10, and 20 MW wind turbines is explained. Next, the construction of the scaling trends using the developed wind turbines as scaling data points is discussed and trends for loads, mass, and cost are presented. Next, the design challenges of larger wind turbines using the developed scaling trends are identified and discussed. Finally, conclusions on the economic viability of existing wind turbine upscaling are discussed.

2. Classical upscaling methods

To examine the effect of size on the design, two different methods are frequently used. First, the analytic relation between a number of important parameters that govern the design can be formulated as a function of rotor diameter (or radius) by assuming that all geometrical parameters vary linearly with size [27,28]. This approach is called the analytic scaling law (also known as the similarity or linear scaling rule). Appendix A gives a detailed overview of the method.

Analytic scaling enables the realization of scaling trends based on wind turbines that are not size optimized, and that may not meet all design constraints. Therefore, the usage of this method is limited to the conceptual design phase [29]. This makes the method less suited for studying detailed technical and economical characteristics, in which the optimized end results are important.

Second, parameters of interest can be statistically correlated to rotor diameter using the existing wind turbines' data. In this approach, real data are viewed collectively, and scaling trends are developed by correlating these data [30]. As an example, Fig. 1 shows the correlation of the rated power output of 27 wind turbines to rotor diameter in the range of 15–130 m.

In this figure, the curve fit to the data points shows almost a square relation with size, and to study wind turbines that are larger than existing ones, the curve can be extrapolated. However, extrapolation beyond the data range introduces uncertainty in the results, which is considered to be the main drawback of this technique. Furthermore, the data points used to develop the scaling trends are obtained with wind turbines of different concepts and design assumptions, and this introduces scattering in the data points.

To overcome the drawbacks of these two methods, the present paper develops a novel method where for several given scales of interest, optimized wind turbines are developed. Based on these optimized designs, the relation between different parameters and rotor diameter can be extracted and used to develop more accurate trends [31,32]. This method is explained in the next section.

3. Development of large scale wind turbines

The design of a wind turbine operating in a wind farm is a complex decision making process [33]. To facilitate the understanding of the work presented in this research, a brief summary of the MDO approach that serves as the basis for the study is presented.

An earlier study showed that the economies of scale are negligible in the rated power range of 0.75–3 MW [34]. To study the challenges and trends of wind turbines beyond the existing 5–7 MW range, technical and economical data of large scale wind turbines are needed. Therefore, the realization of 5, 10, and 20 MW wind turbines is performed using MDO to obtain the required technical and economical data. This section explains how these wind turbines are designed.

3.1. Aeroservoelastic simulation

MDO requires the numerical computation of the objective function and design constraints, using simulations that represent the underlying physics. Among the various simulations that have been developed for the wind energy research community, a series

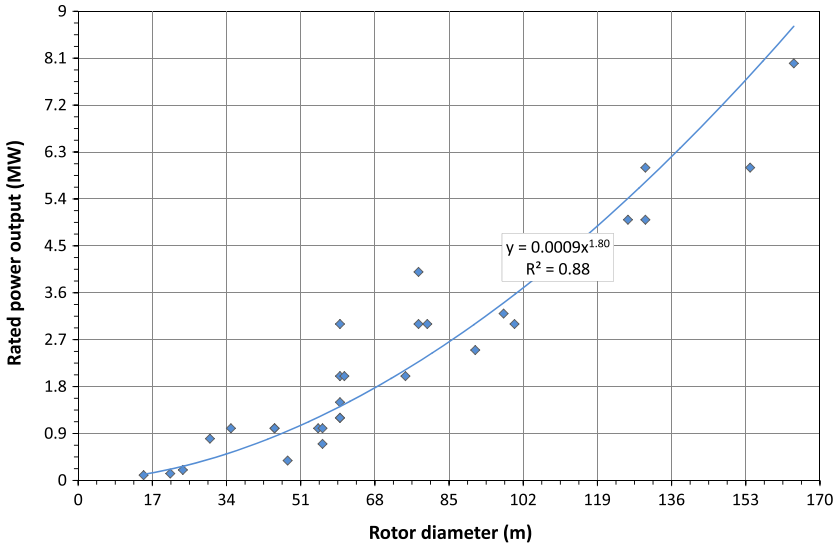

Fig. 1. Rated power output of the wind turbine as a function of rotor diameter. These data are collected by the authors from public product brochures and company web sites. Professional database services also exist to buy these data collectively. (http://www.thewindpower.net/turbines_databases_en.php, last accessed May 22, 2016).

Table 1
Selection of the aeroservoelastic simulation codes.

Tool	Usage
TurbSim	Simulates the 3D turbulent flow field [35]
AeroDyn	Simulates unsteady aerodynamic loads [36]
AirfoilPrep	Corrects 2D airfoil data for 3D effects [37]
FAST	Simulates the dynamic response of the wind turbine [38]
BModes	Computes modal frequencies [39]
Crunch	Processes time domain output data [40]
WindPACT	Models mass and cost of components [41]
Fatigue	Computes fatigue damage [42]

of National Renewable Energy Laboratory (NREL) tools are used as presented in Table 1.

However, these simulators are standalone codes, and the data transfer and process flow among them have to be done by the designer manually. All these standalone codes are coupled to obtain an integrated and automated multidisciplinary analysis that could be linked to an optimization algorithm. Fig. 2 depicts the coupled framework to capture the aeroservoelastic behavior of the wind turbine, and to evaluate the objective function and the design constraints. This coupling is accomplished using a script that controls the data and process flow. More details about the development of this integrated design tool can be found in previous works by the authors [43–46].

3.2. Multidisciplinary design optimization formulation

The majority of large scale wind turbines designed nowadays are upwind, 3-bladed, and pitch-regulated variable-speed turbines, and this is the type of turbine this research focuses on. To make consistent 5, 10, and 20 MW designs and to avoid the scattering of the data points, the 5 MW NREL wind turbine [48] is redesigned and optimized first. In this step, no conceptual change is considered for this design, and the optimized design has exactly the same design details, such as the airfoil type and the controller design. Then, to provide an initial set of design data needed for the optimization to start with, this redesigned wind turbine is upscaled to 10 and 20 MW using linear scaling rules [49]. After this step, time domain aeroservoelastic design optimization of the 10 and 20 MW wind turbines takes place using the same set of design assumptions that were used to redesign the 5 MW wind turbine.

This provides the optimal preliminary data, such as rotor diameter, hub height, rated rotational speed, and structural and aerodynamic design of the tower and rotor. These data are then used to estimate the mass and cost of all the components other than the rotor and tower that yield an optimal design. The FAST aeroservoelastic code is used for the time domain simulation of the wind turbines [38].

A design optimization problem can be mathematically stated as:

$$\text{Find } x = \{x_1, \ldots, x_n\} \text{ that minimizes } f(x), \tag{1}$$

where f is the objective function, and x is the n-dimensional design variable vector, which is subject to lower and upper bounds, as follows:

$$x_{\text{lower}} \leqslant x \leqslant x_{\text{upper}}, \tag{2}$$

This minimization problem is subject to equality and inequality design constraints:

$$h_k(x) = 0, \tag{3}$$

$$g_j\{x\} \geqslant 0, \tag{4}$$

The above functions and variables are now specified for the wind turbine problem of interest to this research.

3.2.1. Design variables

Since the tower and the rotor are the most flexible components of a wind turbine, and their dynamic response governs the design, they are considered as the main components. There are in total 18 design variables for the rotor. These variables are the chord and twist distribution (7 variables: 3 twists and 4 chords), structural thickness distribution (10 variables), and rotor rotational speed (1 variable). For the tower, there are in total 5 design variables. The tower design variables are the height (1 variable), structural thickness at the tower bottom and top (2 variables), and tower diameter at the tower bottom and top (2 variables).

Cubic interpolation for the blade and linear interpolation for the tower are used to find the distributed properties of the blade and tower between these sections, respectively. Upper and lower limits are considered for these variables to define the bounds of the design space.

3.2.2. Design constraints

In addition to the upper and lower bounds of the design variables, several functional design constraints are enforced. These design constraints are nonlinear functions of the design variables, and in total 51 inequality constraints are enforced for the optimization of the rotor and tower. Partial safety factors as recommended by the IEC61400 [50] standard are also considered in these design constraints.

The blade design constraints are stresses and fatigue damage at 5 cross sections along the blade, blade-tower clearance from 9 to 25 m/s, and the first 3 natural frequencies of the isolated blade. Fatigue damage calculation is performed using rain-flow cycle counting based on the stress time-signals, and the Palmgren–Miner rule [51,52]. The tower design constraints are the stresses and fatigue damage at 6 cross sections along the tower, and the first and second natural frequencies. All the design constraints of the blade and tower are continuous and smooth, and therefore differentiable.

3.2.3. Objective function

The objective for each design optimization is to minimize the levelized cost of energy (LCoE) for a given wind turbine [53,54]. The combination of various cost models [41] and the annual energy production (AEP) enable the calculation of LCoE as:

$$\text{LCoE} = \left(\frac{\text{ICC} \times \text{IR} + \text{LRC} + \text{OM}}{\text{AEP}}\right), \tag{5}$$

where IR represents 0.1185 of interest rate [55], and AEP is defined as:

$$AEP \approx 8760 \sum_{i=\text{cut-in}}^{\text{cut-out}} P(V_i) f(V_i), \tag{6}$$

where $P(V)$ is the wind turbine power curve, 8760 is a constant representing the number of hours in a year, and i index shows the wind speed range from the cut-in to cut-out. In this formulation, the wind probability distribution function $f(V)$ is:

$$f(V) = \left(\frac{k}{c}\right)\left(\frac{V}{c}\right)^{k-1} \exp\left[-\left(\frac{V}{c}\right)^{k}\right], \tag{7}$$

where k is the Weibull shape factor, and c is the Weibull speed scale factor. The optimal design of a wind turbine has strong dependency to these parameters [56,57], and in this research, c is 9.47, and k is 2. These are typical values as found in the literature [58,59]. Note that

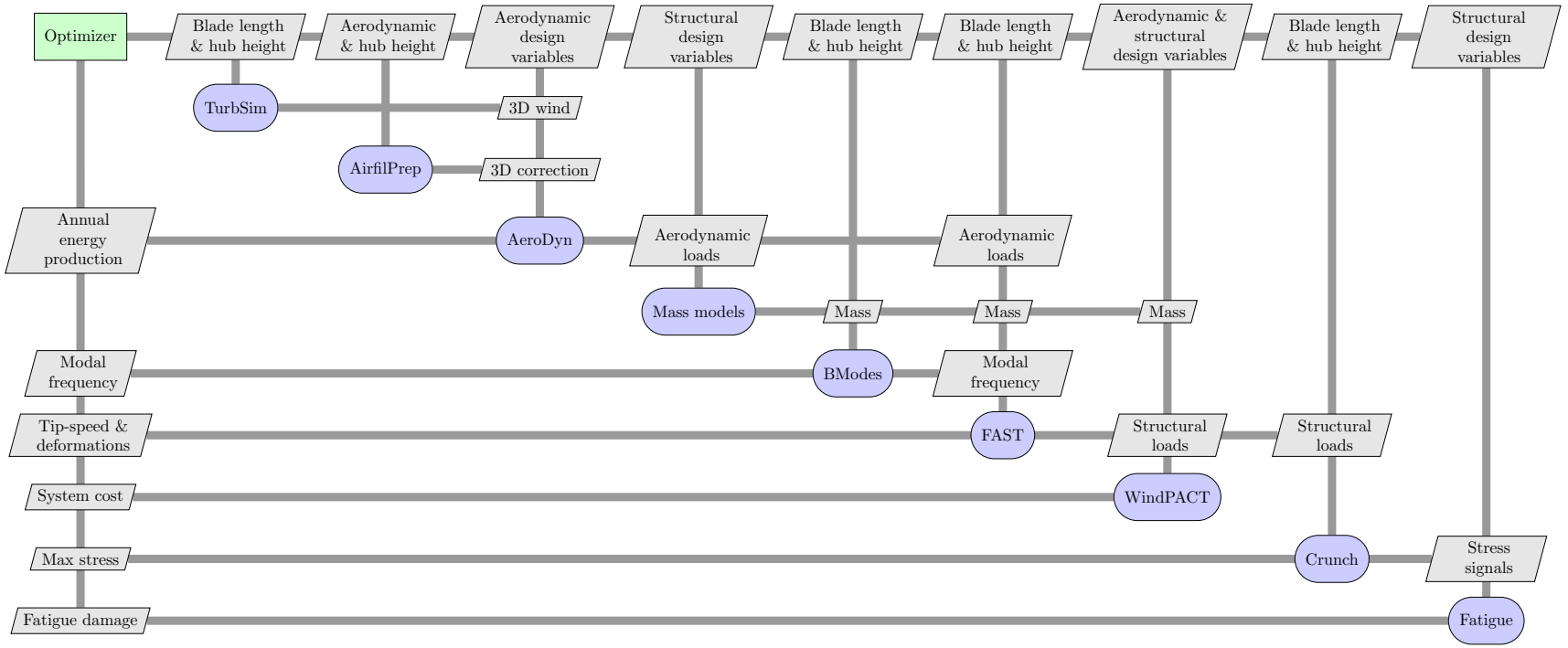

Fig. 2. Extended design structure matrix [47] of the coupled framework to control the process and data of the standalone codes of Table 1. The green box is the optimizer, rounded blue boxes are the standalone simulation, and the gray parallelograms represents the data. The gray lines allow the data flow from top to the bottom, and from left to the right on the upper triangular section, and bottom to the top and right to the left on the lower triangular section. (For interpretation of the references to colour in this figure legend, the reader is referred to the web version of this article.)

Table 2
Cost estimation of the optimized 5, 10, and 20 MW wind turbines in 1000 US Dollar.

Cost	5 MW	10 MW	20 MW
3 Blades	1057.5	2474.9	8570.7
Hub	158.3	324.2	1037.5
Blade pitch system	263.0	664.5	2143.0
Nose cone	14.2	21.8	36.1
Low speed shaft	182.6	499.9	1783.4
Main bearing	71.9	245.2	1151.5
Gearbox	877.2	2085.0	4955.0
Mechanical brake system	11.0	22.2	44.4
Generator	398.0	796.1	1592.2
Power electronics	393.2	786.4	1572.8
Yaw system	160.5	451.2	1665.5
Main frame	172.9	341.8	808.1
Platform and railing	95.1	188.1	444.7
Nacelle cover	73.3	142.1	279.6
Electrical connections	308.8	617.7	1235.5
Cooling and hydraulic system	77.2	154.5	309.0
Safety and condition monitoring	65.3	65.3	65.3
Tower	968.9	3765.6	12497.0
Marinization	722.2	1842.3	5042.5
Turbine capital costs (TCC)	6072.3	15489.0	45618.0
Foundation	2174.7	4349.5	8699.0
Port and staging	144.9	289.9	579.9
Turbine installation	732.8	1465.8	2931.5
Electrical connection	2063.5	4127.0	8253.9
Permits and site assessment	215.5	431.0	862.1
Personnel access equipment	70.2	70.2	70.2
Scour protection	403.0	806.2	1612.3
Decommissioning	403.3	810.8	2058.9
Balance of station (BOS)	5834.9	11539.6	23009.0
Warranty premium	802.5	2047.0	6028.8
Initial capital cost (ICC)	12280.2	29886.4	68627.0
Levelized replacement	99.0	198.0	396.1
Operation and maintenance	664.5	1316.8	2873.7
Interest rate	0.1185	0.1185	0.1185
AEP (GW Hr)	28.397	56.273	122.806
LCoE (USD kW h)	0.0630	0.0641	0.0704

an AEP conversion loss of 5.6% is considered for the mechanical-to-electrical losses in the drive train, similar to the DOWEC design [60].

These cost models are either dependent or independent of the design variables of the blade and tower. Therefore, during the optimization process the value of those dependent models is also indirectly optimized to give an integrated design with the lowest LCoE. An example of a dependent model is the hub mass and cost that does depend on the blade mass. The independent models do not have any size dependency, and therefore fixed for all sizes. The safety system is an example of an independent cost item to size. Details of these models can be found in [61–65].

The quantification of the AEP, the system masses and the costs allows for the LCoE to be calculated and used as a multidisciplinary objective function to be minimized. The solution of this optimization problem results in a wind turbine design that includes rotor and tower data, cost and mass data, and the operational parameters of the wind turbine. These data are then used to develop the scaling trends as explained in the next section. Table 2 presents the cost share of the optimized 5, 10, and 20 MW wind turbines.

Note that these cost models are not intended to yield an exact turbine pricing that is a function of volatile market factors beyond the scope of this research. However, they can provide an accurate projection of the cost based on the existing wind turbine technology to be used in this optimization study. To even better reflect the existing technology, the cost models listed in Table 2 are updated using the producer price index (PPI[4]) to the cost of materials and labor in 2010. The PPI is used by the US Department of Labor to track costs of products and materials as the technology changes over time. Therefore, they represent the existing technology for better cost estimates. These cost models have already been detailed by Fingersh et al. [41].

[4] http://www.bls.gov/ppi/.

Table 3
Gross design data and properties of the optimized 5, 10, and 20 MW wind turbines.

Design specification	5 MW	10 MW	20 MW
Rotor diameter (m)	130	182	286
Rated tip speed (m/s)	88	82	98
Rated rotational speed (RPM)	12.9	8.5	6.5
Gearbox ratio (–)	91	139	180
Cut-in, rated and cut-out wind speed (m/s)	3, 11.4, 25	3, 11.7, 25	3, 10.7, 25
Maximum blade pitch rate (deg/s)	8.0	5.6	4.8
Blade-pitch angle at peak power (deg)	0.0	0.0	0.0
Maximum blade tip-deflection (m)	5.6	7.9	11.8
Hub height (m)	82.4	110.4	162

A variable-speed controller is used for the partial and transition load region, and a full-span rotor-collective blade pitch controller is used for the full load region. The controller is designed after each optimization iteration to guarantee power maximization for the below rated region, and power regulation for the above rated region [66]. Table 3 provides the gross design data and properties for the optimal 5, 10, and 20 MW wind turbines.

4. Development of scaling trends using optimized wind turbines

To study the technical and economical feasibility of larger wind turbines up to 20 MW, it is required to analyze how size impacts the design. This is achieved by developing the loading, mass and cost trends using properties of optimized 5, 10, and 20 MW wind turbines as data points. The optimized wind turbines have the same design concept, which is a 3 bladed, upwind, variable-speed, pitch-regulated, geared design with a tubular tower [67].

In the upscaling literature, scaling trends are developed using power curve fits to the data points by having the rotor diameter as the independent parameter [27,28,30,68]. That is: aR^b, where R is the rotor diameter, a is the curve coefficient, and b is the curve exponent. This research uses the same notation for consistency and ease of comparison with the analytical scaling law, and existing data trends as presented in the literature. However, the true independent parameters for the optimized turbines are their rated powers, for which the rotor diameters are consecutively optimized.

4.1. Loading-diameter trends

This subsection presents the trends of loading versus diameter for the main load carrying components of a wind turbine: blade, low speed shaft and tower. For the loading trends, the trend exponent shows the sensitivity of the loads with respect to size. For the blade and the tower, the loading trends are presented at the blade root and tower base, respectively, where the moments are maximum.

4.1.1. Blade

The blade experiences flapwise loads that are predominantly aerodynamic, and edgewise loads that are mostly due to gravity. Analytic scaling predicts the flapwise bending moments to increase with R^3, and edgewise bending moment with R^4. The prediction using the existing data trend is $R^{2.86}$ for flapwise loads, and $R^{3.25}$ for edgewise loads as presented in Figs. 3 and 4, respectively. Loading-diameter trends using the optimized designs are $R^{2.62}$ for flapwise bending moment, and $R^{3.41}$ for the edgewise bending moment. The lower exponent for the existing data trend for

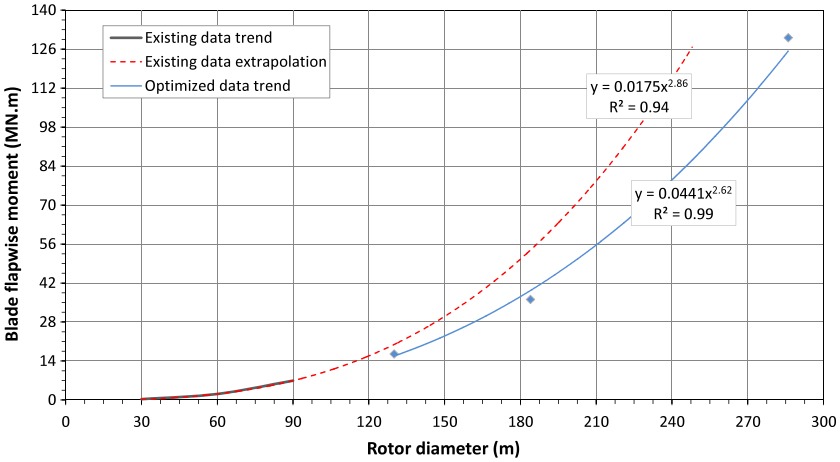

Fig. 3. Upscaling of blade flapwise loads from 5 to 20 MW to show the increase of aerodynamic loads.

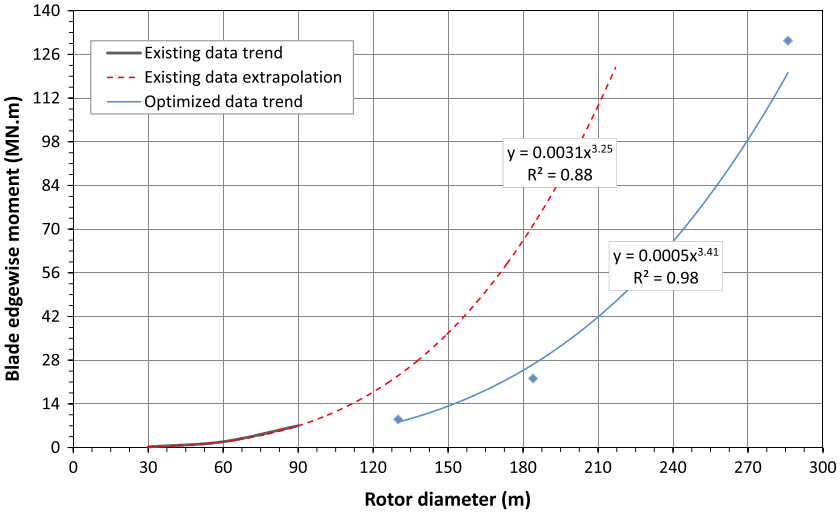

Fig. 4. Upscaling of blade edgewise loads from 5 to 20 MW to show the increase of gravity loads.

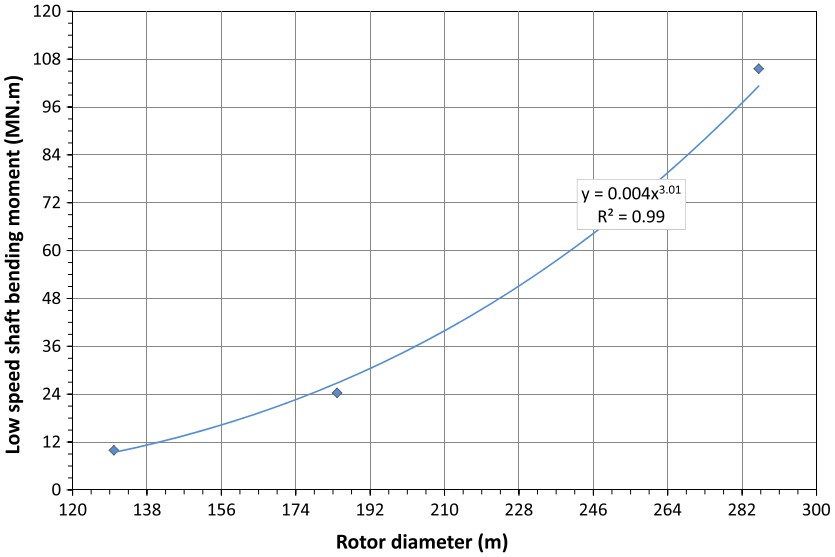

Fig. 5. Upscaling of low speed shaft bending moment from 5 to 20 MW reflecting the increase of gravity loads using the optimized wind turbine data.

edgewise loads might be due to the use of data for smaller turbines, where the aerodynamic loads are still significant when compared to gravity loads. Note that the existing data trends in the figures are extrapolated to allow comparison with the optimized data trends beyond their range.

Although, the two classical upscaling methods show some level of inaccuracy compared to the optimized data trends, they all agree that the edgewise loads increase more rapidly than the flapwise loads. This means that the gravity loads have a more negative influence on the design compared to aerodynamic loads, and it will dominate the blade design at larger scales [69].

4.1.2. Low speed shaft

For the low speed shaft both the bending and torsional moment influence the design. Shaft bending moment is mass driven and scales with R^4 using analytic scaling, and $R^{3.01}$ for the optimized wind turbines. This is shown in Fig. 5. There is no published data in the literature for the existing data trends.

Shaft torsional moment is aerodynamically driven, and it scales with R^3 using analytic scaling. The optimized data trend predicts an increase with $R^{3.03}$ as depicted in Fig. 6. Also, no data trends have been found in the literature for the shaft torsional moment.

4.1.3. Tower

The tower experiences fore-aft, side-to-side, and torsional moments. The tower fore-aft bending moment scales with R^3 for the analytic scaling, with $R^{2.33}$ using extrapolation from the existing data, and with $R^{2.92}$ for the optimized designs.

As Fig. 7 shows, the existing data extrapolation exhibits a smaller value of the trend exponent compared to the optimized data. This is due to the scattering of the data points in the existing data trends (not shown due to protect intellectual property). The quality of the correlation between two data sets is measured by the *R*-squared value. *R*-squared is a statistical measure showing the effectiveness of the rotor diameter in forecasting the fore-aft bending moment. $R = 1.0$ means the correlation is considered 100%, and $R = 0.0$ means no correlation exists. Therefore, the large spread of the data reduces *R* to 0.71.

Fig. 8 shows the side-to-side bending moment that scales as $R^{4.19}$ for the optimized design. This is considerably larger than

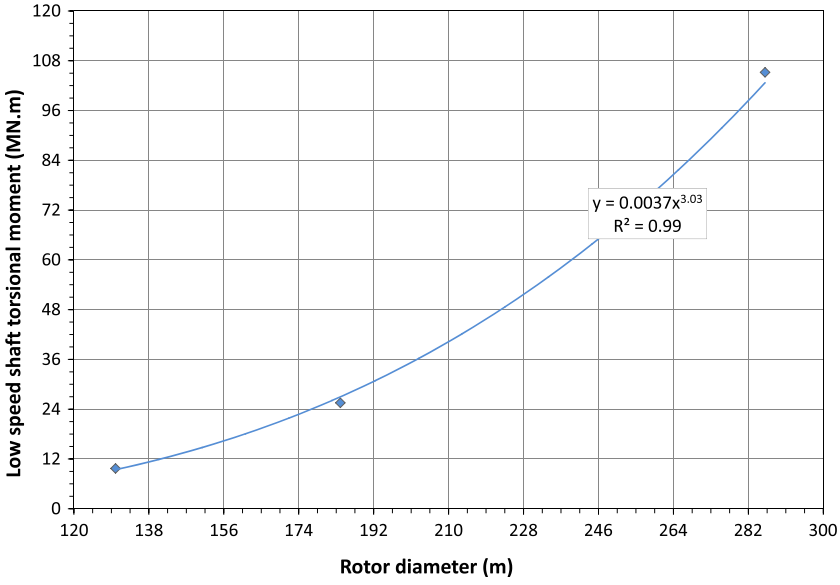

Fig. 6. Upscaling of low speed shaft torsional moment from 5 to 20 MW reflecting the increase of rotor torque using the optimized wind turbine data.

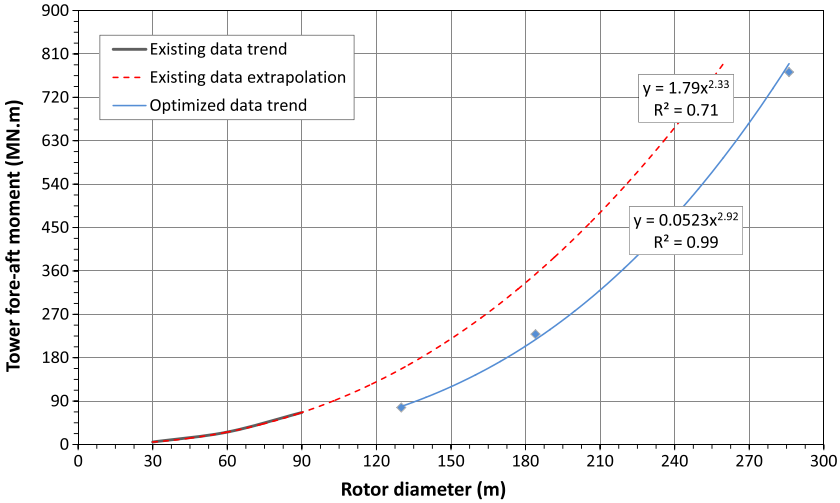

Fig. 7. Upscaling of the tower fore-aft bending moment from 5 to 20 MW corresponding the increase of rotor thrust.

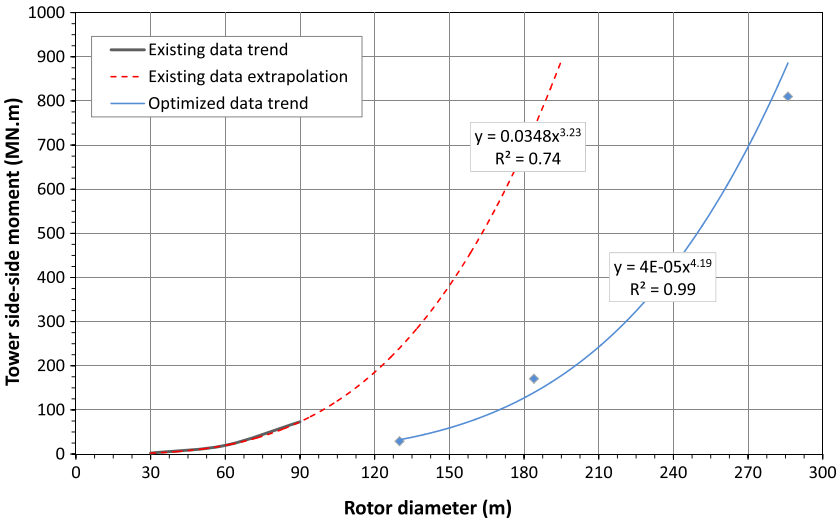

Fig. 8. Upscaling of the tower side-to-side bending moment from 5 to 20 MW showing the increased dynamic amplification of loads.

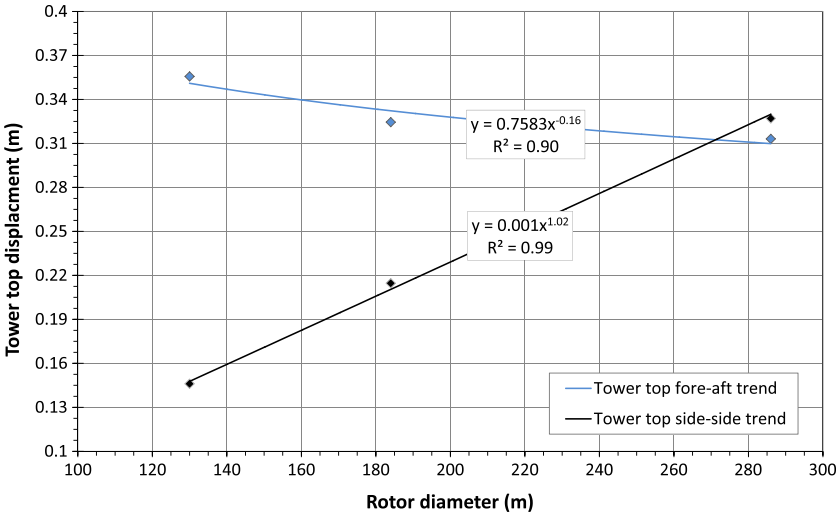

Fig. 9. Upscaling of the tower top side-to-side bending motion from 5 to 20 MW showing the increased flexibility of the system.

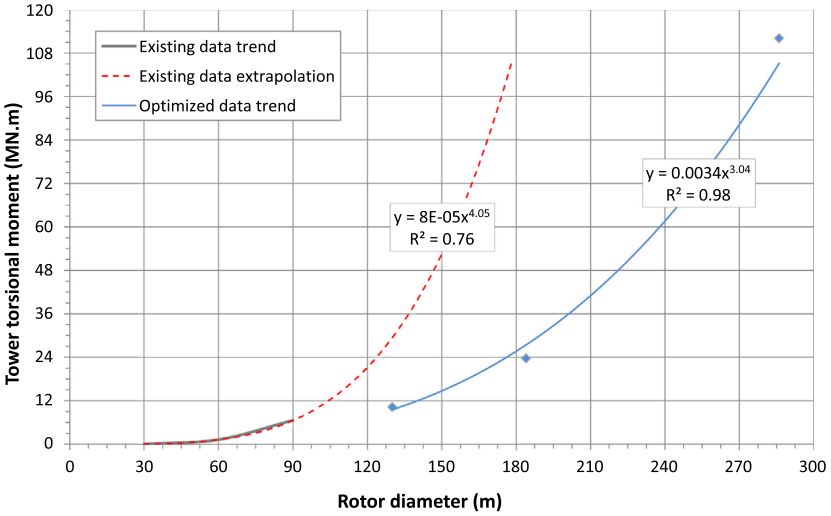

Fig. 10. Upscaling of the tower torsional moment from 5 to 20 MW showing mismatch of the existing data trend with optimized and analytic scaling.

Table 4
Comparison of loading-diameter trends of the tower using different scaling methods.

Scaling method	Fore-aft	Side-to-side	Torsional
Analytic scaling	R^3	R^3	R^3
Existing data extrapolation	$R^{2.33}$	$R^{3.23}$	$R^{4.05}$
Optimized data trend	$R^{2.92}$	$R^{4.19}$	$R^{3.04}$

the R^3 trend in analytic scaling, and $R^{3.23}$ when using existing data trends. This shows that the side-to-side loads are dynamically more amplified at larger scales.

This can also be recognized when looking at the side-to-side motion in Fig. 9. As depicted in the figure, the side-to-side motion of the tower top increases more rapidly, while the tower top fore-aft motion decreases. This behavior can act as a design bottleneck for larger wind turbines due to the fact that the side-to-side motion has little aerodynamic damping. Passive and active means of motion control is needed to overcome this problem [70,71].

Fig. 10 shows a good agreement for the tower torsional moment trends between the optimized wind turbines ($R^{3.04}$) and analytic scaling (R^3). There is, however, a mismatch with the existing data trend ($R^{4.05}$). Also in this case the R-squared value indicates a lower correlation.

As stated by Jamieson [72] the effect of turbulence in generating differential loading on the rotor plane causes a yaw-torque that is responsible for the increase observed in the existing data trend. However, such a mechanism is not observed in the results of this research. Table 4 summarizes the loading-diameter trends of the tower.

4.2. Mass-diameter trends

This section presents the mass-diameter trends of the blade and tower, and their mass share compared to the total mass of the system.

4.2.1. Blade

Fig. 11 shows the mass trend of the optimized blades that scales with $R^{2.64}$. The mass trend using analytic scaling is R^3, and $R^{2.09}$ for

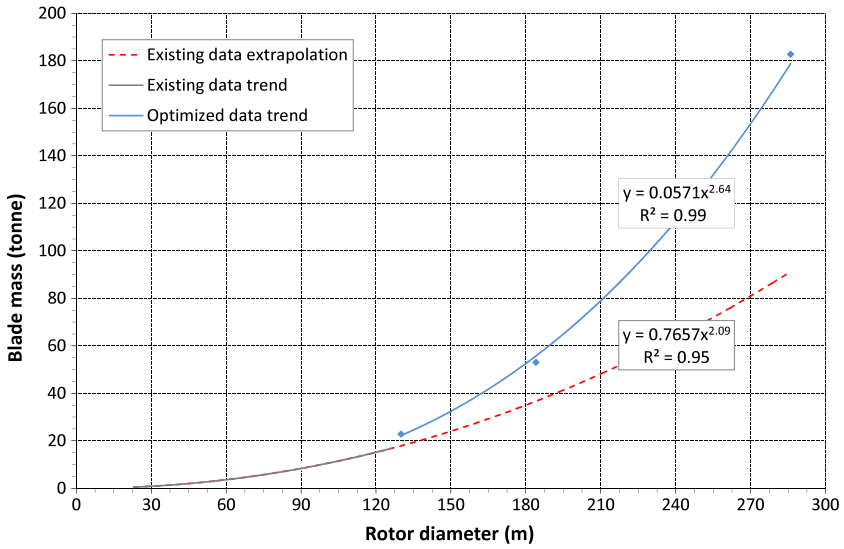

Fig. 11. Scaling of a single blade mass from 5 to 20 MW showing the negative influence of upscaling.

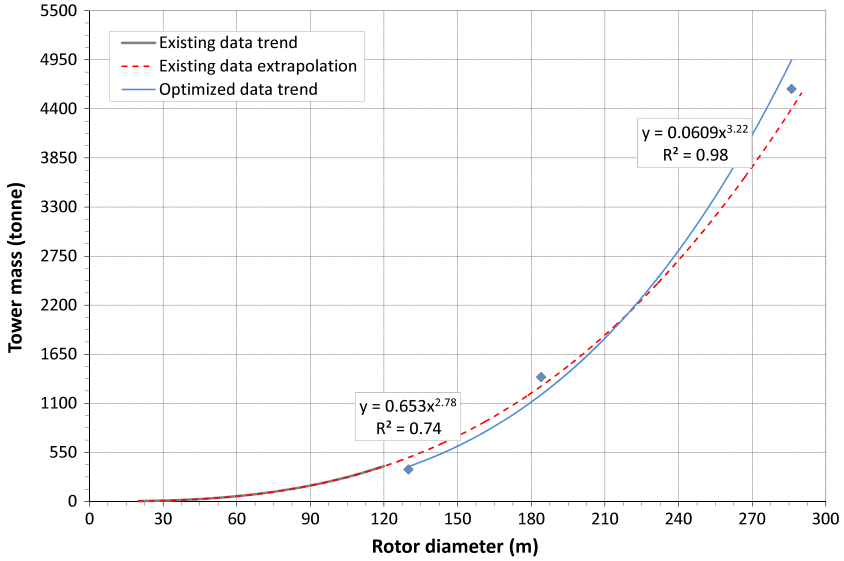

Fig. 12. Upscaling of the tower mass from 5 to 20 MW showing the effect of linearly varying thickness and diameter of the optimized design.

the existing data. Compared to the existing data trend, the optimized data indicates that upscaling with the same materials and concepts negatively influences the design. The lower exponent for the existing data trend may be caused by technology changes that combat the mass increase (e.g., improvements in load control from stall to collective pitch to cyclic pitch).

4.2.2. Tower

Fig. 12 shows the scaling of the tower mass with $R^{2.78}$ using the existing data, and $R^{3.22}$ for the optimized data. The value using the analytic scaling is R^3. The optimized trend shows a higher mass increase compared to the two classical methods. The reason for such a difference can best be explained when looking at the mass share at different scales as presented in the next subsection.

4.2.3. Mass share at different scales

Fig. 13 shows the mass share of the blade and tower with respect to the remaining components of the wind turbine. Engineering models as presented in the WindPACT study are used to have an accurate estimate of the mass of components other than the blade and tower [41]. This includes the mass of the following components: bed-plate, gearbox, hub, low speed shaft, generator, pitch system, pitch bearing, platform and railing, main bearing, high speed shaft and brake, nose cone, hydraulic and cooling, nacelle cover, yaw system, and foundation.

As the figure shows, the mass share of the tower increases from 55.4% at 5 MW to 70.6% at 20 MW. This is consistent with the large scale exponents observed for the tower bending and torsional moments. Therefore, tower top mass reduction and load alleviation is an emerging need for large scale wind turbines.

4.3. Cost-diameter trends

Wind turbine design is a complex multidisciplinary task, and a technical improvement in one discipline requires to study its effect on other disciplines as well. As an example, increasing the blade length to have higher annual energy production (aerodynamic improvement) increases the loads at the blade root in turn (negative structural effect). Therefore, if the proposed improvement does not overcome all the negative effects, then it will end up with a negative overall impact.

Considering these facts, a multidisciplinary merit index is needed to evaluate the overall impact of any single disciplinary improvement. The LCoE is a multidisciplinary merit index that couples different disciplines and allows the system evaluation of any design improvement. Therefore, this paper uses LCoE to investigate the overall impact of upscaling on the design. Unfortunately, no comparison could be made with the analytic scaling, and existing data. For the analytic scaling no formulation can be made to correlate the size to cost. For the existing data, manufacturers treat cost information confidential due to the market competitiveness.

Cost models presented in the WindPACT study are used in this study to have an estimate of the cost of components other than the blade and tower [41]. These include the cost models for hub, pitch mechanism and bearings, nose cone, low speed shaft and bearings, gearbox, mechanical brake, high speed shaft and coupling, generator, power electronics, yaw drive and bearing, main frame, electrical connections, hydraulic system, cooling system, nacelle cover, control equipment, safety system, condition monitoring, tower, and marinization (extra cost to protect against marine environment like salty water).

Fig. 14 shows the cost breakdown of blade and tower compared to the total cost of the machine. For the blades, the cost share increases from 7.7% at 5 MW to 10.7% at 20 MW, and for the tower, the cost share increases from 7.0% at 5 MW to 15.6% at 20 MW. The exponent of a power curve fit to these cost elements is given in Table 5. As presented in the table, the tower experiences the highest cost impact followed by the yaw system, low speed shaft and blade. This means that upscaling influences more negatively the tower cost compared to other components. Note that in this table some cost elements have the same trend exponent, because they are a function of the rated power, and therefore they have the same trend exponent.

The influence of upscaling on the Turbine Capital Cost (TCC) and Balance of Station (BOS) is depicted in Fig. 15. The TCC consists of the following cost elements: blades, hub, pitch mechanism and bearings, nose cone, low speed shaft and bearings, gearbox, mechanical brake, high speed shaft and coupling, generator, power electronics, yaw drive and bearing, main frame, electrical connections, hydraulic system, cooling system, nacelle cover, control equipment, safety system, condition monitoring, tower, and marinization. The BOS includes the following cost elements: monopile, port and staging equipment, turbine installation, electrical interface and

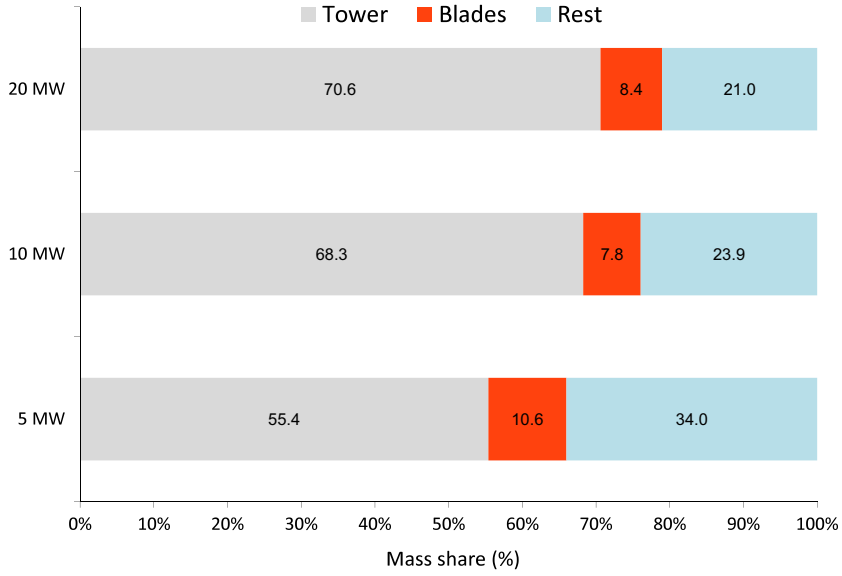

Fig. 13. Mass breakdown of components from 5 to 20 MW showing how upscaling influences blade and tower mass.

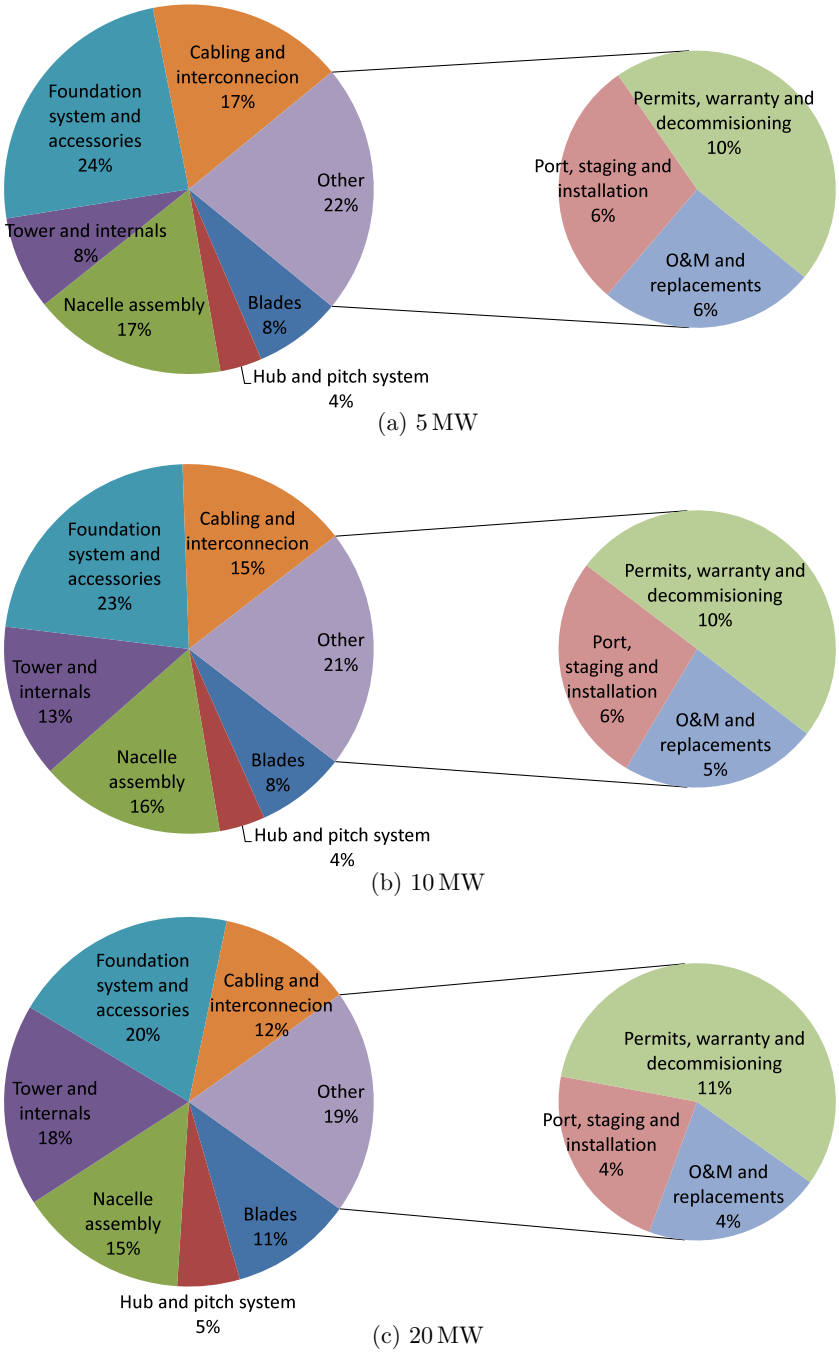

Fig. 14. Cost share for the optimized 5, 10, and 20 MW wind turbines shows the dramatic increase of tower cost with upscaling.

Table 5
Exponent of the curve fit for 5 to 20 MW wind turbines, the higher the exponent the higher the negative impact of upscaling.

Cost component	Trend exponent	Cost component	Trend exponent
Tower	3.22	Electrical interface	1.75
Yaw system	2.97	Installation	1.75
Main shaft	2.89	Scour protection	1.75
Blades	2.66	Generator	1.75
Pitch system	2.66	Power electronics	1.75
Warranty	2.55	Electrical connection	1.75
Marinization	2.55	Engineering	1.75
Main bearing	2.44	Port and staging	1.75
Hub	2.39	Levelized replacement	1.75
Decommissioning	2.22	Hydraulic and cooling	1.75
Gearbox	2.19	HSS and brake	1.75
Bedplate	1.95	Nacelle cover	1.69
Railing and platform	1.95	Hub cone	1.18
Operation and maintenance	1.85	Access equipments	Fixed
Foundation system	1.75	Safety and control	Fixed

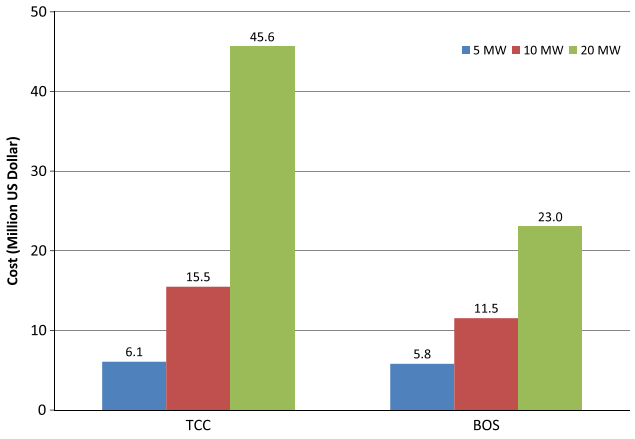

Fig. 15. TCC and BOS for the optimized 5 to 20 MW wind turbines show a rapid increase in TCC.

connections, permits, engineering, site assessment, personnel access equipment, scour protection, transportation, offshore warranty premium, and decommissioning.

TCC and BOS are almost the same for the 5 MW design, but during upscaling the TCC increases more than the BOS. This requires a careful consideration of the TCC during upscaling to cut the costs down.

The advantage of upscaling is the increase of the AEP, and its disadvantage is the increase in the Initial Capital Cost (ICC) that is built up from TCC and BOS. This is presented in Fig. 16, where a trade-off is made between the ICC and AEP. The 1.29 trend exponent of the AEP as an advantage of upscaling does not balance out the 1.57 trend exponent of the ICC. In turn, this negatively influences the LCoE shown in Fig. 17, with a trend exponent increase of 0.14.

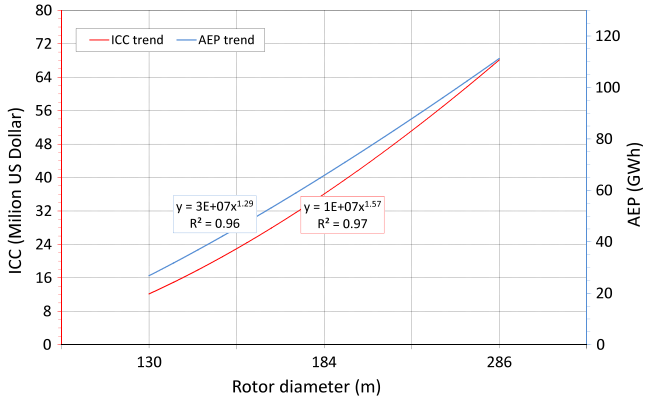

Fig. 16. ICC and AEP trade-off for upscaled wind turbines from 5 to 20 MW shows how upscaling impacts the costs.

5. Challenges of larger wind turbines

In this research, the influence of upscaling on the design and economical characteristics of large wind turbines was studied. This has been done using loading, cost, and mass-diameter trends. These trends were a function of rotor diameter to reflect properly the size dependency. Blade, main shaft, and tower were investigated carefully, because they are the main load carrying, and the most flexible components of a wind turbine.

Loading trends show that the edgewise moment of the blade increases more rapidly than the flapwise moment. This indicates that gravity driven loads are more important to consider than the aerodynamic driven loads as the size increases. In the case of the tower, the side-to-side bending moment exhibits a higher sensitivity to upscaling compared to the fore-aft moment. This is an important design consideration, since the side-to-side motion has little aerodynamic damping, and any misalignment, e.g., due to wind veer or lateral waves, could cause substantial structural damage.

Referring to the mass-diameter scaling trends, the design suffers from the excessive mass growth of the rotor-nacelle assembly. The mass of the rotor causes progressively the mass increase of its supporting components: main bearing, yaw system, and tower. The major reasons for the excessive mass increase of the blade are: maintaining the required blade-tower clearance to prevent hitting the tower in the upwind design configuration, and the required strength against the edgewise loads that are gravity driven. Therefore, additional material in the construction of the blade is needed, which cascades a mass increase of other supporting components of the blade such as main bearing and tower. Any future design must therefore resolve the conflict between higher stiffness needed to have the desired blade-tower clearance, and the low mass needed to reduce edgewise loads of the blade. In such a situation, design

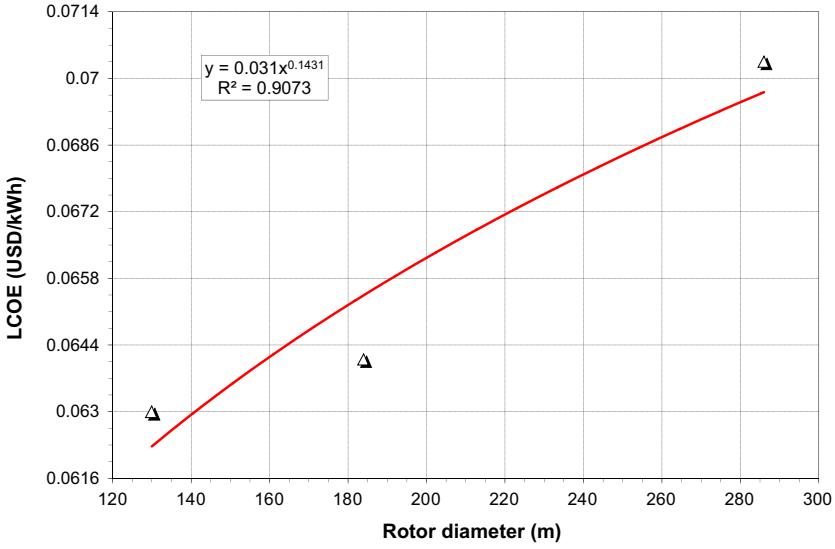

Fig. 17. Trend of LCoE for wind turbines ranging from 5 to 20 MW, showing the overall negative impact of upscaling.

options would be the application of lightweight materials such as carbon fiber reinforced composites to reduce edgewise blade loads, downwind concepts to alleviate the blade tower clearance, and a flexible two-bladed rotor to reduce the tower top mass and loads.

The mass and cost of the tower are also influenced negatively by upscaling. The two main reasons are higher loads, and as mentioned above, the mass of the tower top components. To overcome these problems, load alleviation and mass reduction are considered essential for larger towers. Additionally, active and passive load alleviation techniques are needed to control the motion of the tower side-to-side loads, and to add damping to decay misaligned wind-wave loading in offshore applications.

From a cost point of view, the tower has the highest trend exponent, followed by the yaw system, low speed shaft and the blades. Comparison between the TCC and BOS shows a higher increase of the TCC during upscaling. Furthermore, the trade off between the ICC and annual energy production shows that the extra captured energy by larger wind turbines is not enough to balance out the ICC. This in turn causes the increase of the LCoE.

These results show that upscaling without changing the chosen concept does not lead to a reduction in the costs. It is therefore suggested that a conceptual change in the design of large wind turbines is needed to compensate for the negative effect of upscaling on the design and costs. This conceptual change should target the load and mass reduction of large scale wind turbines to reduce the costs. Two-bladed downwind turbines may reduce the disadvantages of upscaling that are observed for the three-bladed upwind turbine of this study, since the downwind rotor reduces the effect of tower-clearance on rotor mass [73,74]. This, in turn, mitigates the loads. Furthermore, a two-bladed design is potentially lighter compared to a three-bladed design and this reduces the overall system mass. The lower aerodynamic efficiency of a two-bladed design (1–3% lower [75]) reduces the AEP, but this may pay off by having a lighter design and loads. Additionally, in a two-bladed design the transportation and installation costs are lower [63].

Several other alternative design concepts can also be beneficial for large scale designs, such as: segmented, smart, and folding wind turbine blades for mass reduction and easier transportation [76–78], new control algorithms for load alleviation and better power regulation [79–82], and novel grid integration algorithms for better and higher penetration [83–85].

6. Conclusion

Referring to the results of this research, it can be concluded that upscaling without changing the concept, materials, and technology is not viable. The relatively small increase in costs for the balance of station still gives an incentive for upscaling, but this is counteracted by a large increase in the costs of the rotor-nacelle assembly.

Upscaling only can remain an effective cost reduction strategy, if it is associated with some conceptual changes. It also needs to be performed in smaller scaling steps with the introduction of advanced technologies to minimize the negative overall impact of every step. Therefore, upscaling needs to be done in incremental steps to allow the mitigation of negative impacts by advancing the current technology and design methods. Otherwise, upscaling using existing materials and design concepts will result in massive wind turbines that are economically inferior to the existing state of the art.

The scaling observed in data of existing wind turbines is generally more benign than the scaling observed in this study. This is associated with the technology improvements in existing turbines, which have gone hand-in-hand with the increase in turbine size. It would be worthwhile to investigate whether the application of such technology improvements to smaller scale turbines might also increase their economical value.

Acknowledgments

This research was part of the UpWind project supported by the European Union sixth framework program, Grant No. 019945 (2006–2011). The financial support is greatly acknowledged.

Appendix A

The analytic scaling laws presented earlier can be used to obtain an initial design for the 10 and 20 MW wind turbines needed for optimization. These laws not only can describe the dependency of turbine properties to rotor diameter, but they can also be employed to obtain the design properties of an unknown turbine with respect to a known turbine. This is explained by the following equation:

$$\frac{P_x}{P_a} = \frac{0.5C_p^x \cdot \rho_x \cdot \pi \cdot r_x^2 \cdot V_x^3}{0.5C_p^a \cdot \rho_a \cdot \pi \cdot r_a^2 \cdot V_a^3}, \tag{8}$$

where subscript a and x refer to a known and unknown turbine, using the following parameters:

P	Power output
C_p	Power coefficient
ρ	Air density
r	Rotor radius
V	Hub height wind speed

This research assumes the power coefficient and air density of the unknown wind turbine to be the same as the known turbine. Knowing the dependency of the hub height wind speed to the rotor radius as $V \approx r^{\alpha}$ (with α as the wind shear), and replacing that in Eq. (8) yields:

$$\frac{P_x}{P_a} = \frac{r_x^2 \cdot r_x^{3\alpha}}{r_a^2 \cdot r_a^{3a}} = \frac{r_x^{2+3\alpha}}{r_a^{2+3\alpha}}, \tag{9}$$

or:

$$r_x = r_a \cdot \sqrt[2+3\alpha]{\frac{P_x}{P_a}}, \tag{10}$$

The only unknown variable in Eq. (10) is the rotor radius of the unknown turbine, because the designer has already selected the power output of interest to design the unknown wind turbine for. In this formulation, the ratio of the rotor radius between the unknown and the known turbine is defined as the scaling ratio (SR). The SR can be used to obtain any design parameters of interest for the unknown turbine based on the known turbine as:

$$Q_x = Q_a \cdot (SR)^{SF}, \tag{11}$$

where Q is a design parameter for both the known and unknown turbine, and SF is the scaling factor based on the analytic scaling.

References

[1] Klaassen G, Miketa A, Larsen K, Sundqvist T. The impact of R&D on innovation for wind energy in Denmark, Germany and the United Kingdom. Ecol Econ 2005;54(2):227–40.
[2] Blanco MI. The economics of wind energy. Renew Sustain Energy Rev 2009;13(6):1372–82.
[3] BoroumandJazi G, Rismanchi B, Saidur R. Technical characteristic analysis of wind energy conversion systems for sustainable development. Energy Convers Manage 2013;69:87–94.

[4] McGinn D, Green D, Taylor R, et al. Global status report. Tech Rep; Renewables; 2013.
[5] Hepbasli A. A key review on exergetic analysis and assessment of renewable energy resources for a sustainable future. Renew Sustain Energy Rev 2008;12(3):593–661.
[6] McKenna R, Hollnaicher S, Fichtner W. Cost-potential curves for onshore wind energy: a high-resolution analysis for Germany. Appl Energy 2014;115:103–15.
[7] Cheng M, Zhu Y. The state of the art of wind energy conversion systems and technologies: a review. Energy Convers Manage 2014;88:332–47.
[8] Lantz E, Wiser R, Hand M. The past and future cost of wind energy. Tech Rep; National Renewable Energy Laboratory, Golden, CO, Report No. NREL/TP-6A20-53510; 2012.
[9] Islam M, Mekhilef S, Saidur R. Progress and recent trends of wind energy technology. Renew Sustain Energy Rev 2013;21:456–68.
[10] Kaldellis JK, Zafirakis D. The wind energy (r)evolution: a short review of a long history. Renew Energy 2011;36(7):1887–901.
[11] Joselin Herbert G, Iniyan S, Sreevalsan E, Rajapandian S. A review of wind energy technologies. Renew Sust Energy Rev 2007;11(6):1117–45.
[12] Bulder B, Hendriks H, van Langen P, Lindenburg C, Snel H, Bauer P, et al. The ICORASS feasibility study, final report. Tech Rep; Energy Center Nederland, ECN-E-07-010; 2007.
[13] Purvins A, Zubaryeva A, Llorente M, Tzimas E, Mercier A. Challenges and options for a large wind power uptake by the european electricity system. Appl Energy 2011;88(5):1461–9.
[14] Conti JJ, Holtberg PD, et al. Annual energy outlook 2014. Tech Rep; Energy information association, Report No, DOE/EIA-0383; 2014.
[15] Berry D. Innovation and the price of wind energy in the US. Energy Policy 2009;37(11):4493–9.
[16] Afanasyeva S, Saari J, Kalkofen M, Partanen J, Pyrhönen O. Technical, economic and uncertainty modelling of a wind farm project. Energy Convers Manage 2016;107:22–33.
[17] Ashuri T, Zhang T, Qian D, Rotea M. Uncertainty quantification of the levelized cost of energy for the 20mw research wind turbine model. In: AIAA Science and Technology Forum and Exposition (SciTech), Wind Energy Symposium. San Diego, California: American Institute of Aeronautics and Astronautics; 2016. p. 1–11.
[18] Díaz G, Gómez-Aleixandre J, Coto J. Dynamic evaluation of the levelized cost of wind power generation. Energy Convers Manage 2015;101:721–9.
[19] Capponi PAC, Ashuri T, van Bussel GJW, Kallesøe B. A non-linear upscaling approach for wind turbine blades based on stresses. In: European wind energy conference and exhibition. Brussels, Belgium: The European wind Energy Association; 2011. p. 1–8.
[20] Sieros G, Chaviaropoulos P, Sørensen JD, Bulder B, Jamieson P. Upscaling wind turbines: theoretical and practical aspects and their impact on the cost of energy. Wind energy 2012;15(1):3–17.
[21] Hendriks B. Upscaling: consequences for concepts and design. In: The European wind energy association, Brussels, Belgium; 2008, p. 1–20. Workshops Track, Session Code: CP2.
[22] Veers P, Ashwill TD, Sutherland HJ, Laird DL, Lobitz DW, Griffin DA, et al. Trends in the design, manufacture and evaluation of wind turbine blades. Wind Energy 2003;6(3):245–59.
[23] Griffith DT, Ashwill TD. The sandia 100-meter all-glass baseline wind turbine blade: Snl100-00. Tech Rep; Sandia National Laboratories, SAND2011-3779, Albuquerque; 2011.
[24] Ashuri T, Zaaijer M. The future of offshore wind turbines. In: 3rd PhD seminar on wind energy in Europe. Pamplona, Spain: European Academy of Wind Energy; 2007. p. 1–7.
[25] Höyland J. Challenges for large wind turbine blades PhD thesis. Norwegian University of Science and Technology; 2010.
[26] Martins JRRA, Lambe AB. Multidisciplinary design optimization: a survey of architectures. AIAA J 2013;51:2049–75. http://dx.doi.org/10.2514/1.J051895.
[27] Chaviaropoulos P. Similarity rules for wind turbine upscaling. Internal report; UPWIND; 2007.
[28] Sieros G, Chaviaropoulos P. Aspects of upscaling beyond similarity. In: The science of making torque from wind, Crete, Greece. 2010, p. 1–10.
[29] Nijssen R, Zaaijer M, Bierbooms W, Van Kuik G, Van Delft D, van Holten T. The application of scaling rules in up-scaling and marinisation of a wind turbine. In: European wind energy conference and exhibition, Copenhagen, Denmark; 2001. p. 619–22.
[30] Jamieson P. Innovation in wind turbine design. John Wiley and Sons; 2011.
[31] Dykes K, Damiani R, Felker F, Graf P, Hand M, Meadows R, et al. Systems engineering applications to wind energy research, design, and development. Tech Rep; US Dept. Energy, Washington, DC, USA, Tech. Rep. NREL/PO-5000-54717; 2012.
[32] Dykes K, Ning A, King R, Graf P, Scott G, Veers P. Sensitivity analysis of wind plant performance to key turbine design parameters: a systems engineering approach. In: 32nd ASME wind energy symposium, National Harbor, Maryland; 2014. p. 1–26.
[33] Lee AH, Hung MC, Kang HY, Pearn W. A wind turbine evaluation model under a multi-criteria decision making environment. Energy Convers Manage 2012;64:289–300.
[34] Lee J, Kim DR, Lee KS. Optimum hub height of a wind turbine for maximizing annual net profit. Energy Convers Manage 2015;100:90–6.
[35] Jonkman B, Buhl M. TurbSim user guide. Tech Rep; National Renewable Energy Laboratory, Rept. NREL/TP-500-41136, Golden, Colorado; 2007.
[36] Laino D, Hansen A. User's guide to the wind turbine dynamics aerodynamics computer software AeroDyn. Tech. Rep.; Windward Engineering LLC, Prepared for the National Renewable Energy Laboratory under Subcontract No. TCX-9-29209-01, Salt Lake City, UT; 2002.
[37] Viterna LA, Janetzke DC. Theoretical and experimental power from large horizontal-axis wind turbines. NASA Technical Report 1982;82.
[38] Jonkman JM, Buhl Jr ML. Fast user guide. Tech Rep; National Renewable Energy Laboratory, Golden, CO, Technical Report No. NREL/EL-500-38230; 2005.
[39] Bir G. BModes user guide. Tech Rep; National Renewable Energy Laboratory, Golden, Colorado; 2007.
[40] Buhl M. Crunch user guide. Tech Rep; National Renewable Energy Laboratory, NREL/EL-500-30122, Golden, CO; 2003.
[41] Fingersh L, Hand M, Laxson A. Wind turbine design cost and scaling model. Tech Rep; National Renewable Energy Laboratory, NREL/TP-500-40566, Golden, Colorado; 2006.
[42] Frendahl M, Rychlik I. Rainflow analysis: Markov method. Int J Fatigue 1993;15(4):265–72.
[43] Ashuri T, Zaaijer MB, Martins JRRA, van Bussel GJW, van Kuik GAM. Multidisciplinary design optimization of offshore wind turbines for minimum levelized cost of energy. Renew Energy 2014;68:893–905. http://dx.doi.org/10.1016/j.renene.2014.02.045.
[44] Ashuri T. Beyond classical upscaling: integrated aeroservoelastic design and optimization of large offshore wind turbines Ph.D. thesis. the Netherlands: Delft University of Technology; 2012.
[45] Ashuri T, Zaaijer MB, van Bussel GJW, van Kuik GAM. An analytical model to extract wind turbine blade structural properties for optimization and up-scaling studies. In: The science of making torque from wind, Crete, Greece. Journal of Physics, Conference series; 2010a, p. 1–7.
[46] Ashuri T, Martins JRRA, Zaaijer MB, van Kuik GA, van Bussel GJ. Aeroservoelastic design definition of a 20 mw common research wind turbine model. Wind Energy 2016. http://dx.doi.org/10.1002/we.1970.
[47] Lambe AB, Martins JRRA. Extensions to the design structure matrix for the description of multidisciplinary design, analysis, and optimization processes. Struct Multidiscip Optim 2012;46(2):273–84.
[48] Jonkman J, Butterfield S, Musial W, Scott G. Definition of a 5-MW reference wind turbine for offshore system development. Tech Rep; National Renewable Energy Laboratory, NREL/TP-500-38060, Golden, CO; 2009.
[49] Ashuri T, Zaaijer MB. Review of design concepts, methods and considerations of offshore wind turbines. In: European offshore wind conference and exhibition. Berlin, Germany: The European Wind Energy Association; 2007. p. 1–10.
[50] IEC61400. Wind turbines, part 3: Design requirements for offshore wind turbines; 2009.
[51] Miner MA. Cumulative damage in fatigue. J Appl Mech 1945;12(3):159–64.
[52] Haghi R, Ashuri T, van der Valk PL, Molenaar DP. Integrated multidisciplinary constrained optimization of offshore support structures. J Phys: Conf Ser 2014;555(1):1–10.
[53] Chehouri A, Younes R, Ilinca A, Perron J. Review of performance optimization techniques applied to wind turbines. Appl Energy 2015;142:361–88.
[54] Mirghaed MR, Roshandel R. Site specific optimization of wind turbines energy cost: iterative approach. Energy Convers Manage 2013;73:167–75.
[55] Baringo L, Conejo A. Wind power investment within a market environment. Appl Energy 2011;88(9):3239–47.
[56] Mohammadi K, Alavi O, Mostafaeipour A, Goudarzi N, Jalilvand M. Assessing different parameters estimation methods of Weibull distribution to compute wind power density. Energy Convers Manage 2016;108:322–35.
[57] Mohammadi K, Mostafaeipour A. Economic feasibility of developing wind turbines in Aligoodarz, Iran. Energy Convers Manage 2013;76:645–53.
[58] Chang TP. Performance comparison of six numerical methods in estimating Weibull parameters for wind energy application. Appl Energy 2011;88(1):272–82.
[59] Morgan EC, Lackner M, Vogel RM, Baise LG. Probability distributions for offshore wind speeds. Energy Convers Manage 2011;52(1):15–26.
[60] Kooijman H, Lindenburg C, Winkelaar D, van der Hooft E. DOWEC 6 MW pre design, Aero-elastic modelling of the DOWEC 6 MW pre-design in PHATAS. Tech Rep; ECN-CX-01-135, Energy Research Center of the Netherlands, Petten; 2003.
[61] Poore R, Lettenmaier T. Alternative design study report: WindPACT advanced wind turbine drive train designs study. Tech Rep; National Renewable Energy Laboratory, NREL/SR-500-33196, Golden, CO; 2003.
[62] Griffin D. WindPACT turbine design scaling studies technical area: composite blades for 80-to 120-Meter Rotor. Tech Rep; National Renewable Energy Laboratory, NREL/SR-500-29492, Golden, CO; 2001.
[63] Smith K. WindPACT turbine design scaling studies technical area 2: turbine, rotor, and blade logistics. Tech. Rep.; National Renewable Energy Laboratory, NREL/SR-500-29439; 2001.
[64] Bywaters G, John V, Lynch J, Mattila P, Norton G, Stowell J, et al. Northern power systems windpact drive train alternative design study report; period of performance: April 12, 2001 to January 31, 2005. Tech Rep; National Renewable Energy Laboratory, NREL/SR-500-35524, Golden, CO; 2004.
[65] Shafer D, Strawmyer K, Conley R, Guidinger J, Wilkie D, Zellman T, et al. Windpact turbine design scaling studies: Technical area 4–balance-of-station cost. Tech Rep; National Renewable Energy Laboratory, NREL/SR-500-29950, Golden, CO; 2001.

[66] Ashuri T, Zaaijer MB, van Bussel GJW, van Kuik GAM. Controller design automation for aeroservoelastic design optimization of wind turbines. In: The science of making torque from wind, Crete, Greece; 2010, p. 1–7.
[67] Muskulus M, Schafhirt S. Design optimization of wind turbine support structures-a review. J Ocean Wind Energy 2014;1(1):12–22.
[68] Molly J. Maximum economic size of wind energy converters. In: The European wind energy association; 1989, p. 1013–6.
[69] Ashuri T, Zaaijer MB. Size effect on wind turbine blade's design driver. In: European wind energy conference and exhibition. Brussels, Belgium: The European wind Energy Association; 2008. p. 1–6.
[70] Lackner MA, Rotea MA. Passive structural control of offshore wind turbines. Wind Energy 2011;14(3):373–88.
[71] Van Wingerden JW, Hulskamp A, Barlas T, Houtzager I, Bersee H, Van Kuik G, et al. Two-degree-of-freedom active vibration control of a prototyped smart rotor. IEEE Trans Control Syst Technol 2011;19(2):284–96.
[72] Jamieson P. Loading and cost trends using certification calculation. Internal report; UPWIND; 2007.
[73] Reiso M, Muskulus M. The simultaneous effect of a fairing tower and increased blade flexibility on a downwind mounted rotor. J Renew Sust Energy 2013;5 (3):033–106.
[74] van Solingen E, van Wingerden JW, Beerens J. Integrated yaw design of a downwind two-bladed wind turbine. In: American Control Conference (ACC). IEEE; 2015. p. 3702–7.
[75] Paul AJ. A comparative analysis of the two-bladed and the three-bladed wind turbine for offshore wind farms Master's thesis. The Netherlands: Delft University of Technology; 2010.
[76] Lu H, Zeng P, Lei L, Yang Y, Xu Y, Qian L. A smart segmented blade system for reducing weight of the wind turbine rotor. Energy Convers Manage 2014;88:535–44.
[77] Xie W, Zeng P, Lei L. A novel folding blade of wind turbine rotor for effective power control. Energy Convers Manage 2015;101:52–65.
[78] Van Wingerden J, Hulskamp A, Barlas T, Marrant B, Van Kuik G, Molenaar D, et al. On the proof of concept of a smart wind turbine rotor blade for load alleviation. Wind Energy 2008;11(3):265–80.
[79] Viveiros C, Melicio R, Igreja J, Mendes V. Performance assessment of a wind energy conversion system using a hierarchical controller structure. Energy Convers Manage 2015;93:40–8.
[80] Nasiri M, Milimonfared J, Fathi S. Modeling, analysis and comparison of TSR and OTC methods for MPPT and power smoothing in permanent magnet synchronous generator-based wind turbines. Energy Convers Manage 2014;86:892–900.
[81] Ashuri T, Rotea M, Xiao Y, Li Y, Ponnurangam CV. Wind turbine performance decline and its mitigation via extremum seeking controls. In: AIAA Science and Technology Forum and Exposition (SciTech), wind energy symposium. San Diego, California: American Institute of Aeronautics and Astronautics; 2016. p. 1–11.
[82] Lu Q, Bowyer R, Jones BL. Analysis and design of coleman transform-based individual pitch controllers for wind-turbine load reduction. Wind Energy 2015;18(8):1451–68.
[83] Tang Y, Bai Y, Huang C, Du B. Linear active disturbance rejection-based load frequency control concerning high penetration of wind energy. Energy Convers Manage 2015;95:259–71.
[84] Wang S, Chen N, Yu D, Foley A, Zhu L, Li K, et al. Flexible fault ride through strategy for wind farm clusters in power systems with high wind power penetration. Energy Convers Manage 2015;93:239–48.
[85] Kesraoui M, Chaib A, Meziane A, Boulezaz A. Using a DFIG based wind turbine for grid current harmonics filtering. Energy Convers Manage 2014;78:968–75.